Side Shear Setup. I: Test Piles Driven in Florida

Paul J. Bullock, M.ASCE[1]; John H. Schmertmann, F.ASCE[2]; Michael C. McVay, M.ASCE[3]; and Frank C. Townsend, F.ASCE[4]

Abstract: The available literature indicates that pile side shear increases almost linearly with the logarithm of time elapsed after driving, sometimes described using a dimensionless setup factor. A test pile program conducted by the University of Florida measured side shear setup (SSS) for up to 4.7 years on five, 457-mm (18-in), square, prestressed, concrete piles driven into coastal plain soils at different sites. Dynamic tests performed during initial driving and two restrikes measured short-term SSS. Osterberg cells, the first installed in driven concrete piles, measured long-term SSS starting within 24 h of driving and continuing with two to five additional, staged tests. Extensive instrumentation, including vibrating wire strain gauges, Marchetti total stress cells, and vibrating wire piezometers, divided the five piles into 28 segments by soil type with horizontal effective stress measurements for 18 of the segments. This paper describes the University of Florida test pile program and its results. A companion paper analyzes the test results and recommends procedures for implementing SSS in design.

DOI: 10.1061/(ASCE)1090-0241(2005)131:3(292)

CE Database subject headings: Driven piles; Skin friction; Shear strength; Pile load tests; Penetration tests; Aging; Time dependence; Time studies.

Introduction

Driven piles often show a significant increase in side shear capacity versus time that many engineers refer to as "setup" or "freeze", abbreviated herein as "SSS" for "side shear setup". However, most engineers do not include SSS in design calculations, thereby losing extra capacity that could result in economic savings through fewer, shorter, or smaller piles. To further investigate and demonstrate long-term SSS, University of Florida (UF) researchers drove five, full-size, concrete piles into a variety of coastal plain soils, including strain gauge, piezometer, and total stress cell instrumentation in each pile. Subsequent Osterberg cell (O-cell) tests, the first performed on driven concrete piles, documented SSS over a period of up to 4.7 years. The UF test program also evaluated changes in horizontal effective stress against the piles, the effects of soil type and initial effective stress (depth), the effect of pore pressure dissipation, and the potential use of in situ tests for predicting SSS.

This paper presents the background, details, and test results of the UF SSS research. A subsequent companion paper (Bullock et al. 2005) analyzes the test results, discusses the use of the standard penetration test (SPT) as a SSS predictor, evaluates stage-testing effects, and provides recommendations for the design use of SSS in practice.

[1]Senior Engineer, GRL Engineers, Inc., 3636 NW 23rd Pl., Gainesville, FL 32605.

[2]Professor Emeritus, Dept. of Civil and Coastal Engineering, Univ. of Florida, 4509 NW 23rd Ave., Suite 19, Gainesville, FL 32607.

[3]Professor, Dept. of Civil and Coastal Engineering, Univ. of Florida, P.O. Box 116580, Gainesville, FL 32611.

[4]Professor, Dept. of Civil and Coastal Engineering, Univ. of Florida, P.O. Box 116580, Gainesville, FL 32611.

Note. Discussion open until August 1, 2005. Separate discussions must be submitted for individual papers. To extend the closing date by one month, a written request must be filed with the ASCE Managing Editor. The manuscript for this paper was submitted for review and possible publication on August 11, 2003; approved on June 26, 2004. This paper is part of the ***Journal of Geotechnical and Geoenvironmental Engineering***, Vol. 131, No. 3, March 1, 2005. ©ASCE, ISSN 1090-0241/2005/3-292–300/$25.00.

Background

Examples of Setup

Most engineers familiar with the driving and testing of piles have observed setup in the field, and the technical literature includes many examples. For two separate Florida Department of Transportation (FDOT) sites in North Florida, Kehoe (1989) observed that within 11 days after driving, the capacity of square prestressed concrete piles driven in mixed cohesive soils increased an average of 58% at one and 200% at the other. Approximately one-half of this increase occurred in the first 100 min. Karlsrud and Haugen (1985) reported a 30% side shear increase in the interval from 6 to 30 days after jacking closed-end pipe piles (diameter 153 mm) into sensitive overconsolidated Norwegian clay. The excess pore pressure around these piles dissipated within six days. They also determined that approximately two-thirds of the measured SSS resulted from the preshearing effect of repeated (staged) tests on the same pile, a significant effect discussed in the companion paper (Bullock et al. 2005).

Fellenius et al. (1989) showed the capacity of steel pipe and H-piles to increase about 50% between tests conducted at 1 and 21 days after the end of driving (EOD) in sandy clay and silty sand. Of particular interest, they showed this effect using both dynamic (stress wave) and static testing, and in both low and high-permeability soil. Tavenas and Audi (1972) documented a 70% capacity increase of hexagonal concrete piles 2 to 3 weeks after the EOD in high-permeability sand. Seidel et al. (1988) reported an 80% capacity increase for dynamic tests performed 7 to

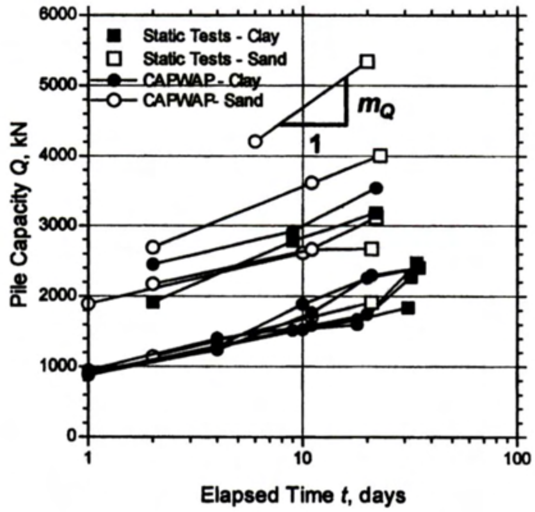

Fig. 1. Pile capacity data from Svinkin et al. (1994)

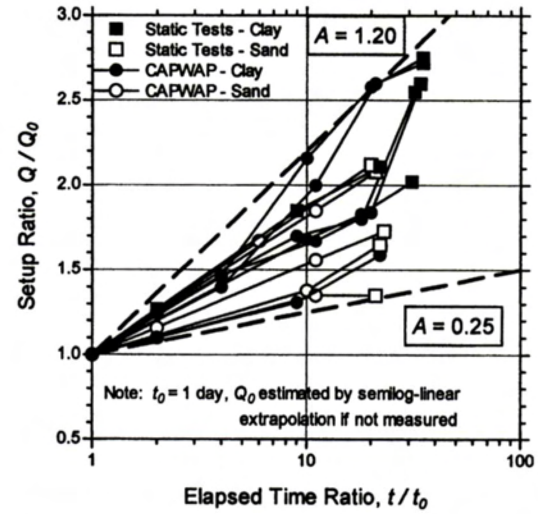

Fig. 2. Setup factor range for Svinkin et al. (1994)

535 days after the EOD for a prestressed concrete pile driven through 12 m of alluvial sands to bear in limestone.

In a few unusual cases, engineers have observed a reduction in pile capacity with time—referred to herein as "relaxation." It occurs primarily because of the dissipation of negative pore pressures created during the pile driving. Chow et al. (1998) identify three stratigraphic profiles that may create this condition: Strong soils that dilate during penetration, weak sedimentary and metamorphic rock, and sands confined by a cofferdam or closely spaced piles. Note that in this research, only 1 of 28 test pile segments showed a long-term capacity decrease, probably due to test conditions and not to relaxation.

Setup Mostly Side Shear

Kehoe (1989) indicates that setup occurs primarily in the side shear against driven piles. Some confusion exists because early researchers often referred to the total pile capacity as "pile bearing capacity"; lumping end bearing and side shear together. Analysis of dynamic tests reported by Samson and Autheir (1986), Skov and Denver (1988), Preim et al. (1989), Kehoe (1989), and Shioi et al. (1992), confirm that end bearing changes little with time. Static tests presented by Airhart et al. (1967) and Axelsson (1998a) also confirm this observation. The writers speculate that the larger shear strains along the sides of the pile compared to below its base cause much more soil destructuring along the sides versus the base, and over a much larger contact area, and that the restructuring recovery produces the SSS. The research described herein measures the pile side shear separately from end bearing, and assumes that any time changes in end bearing have a negligible effect on measured SSS.

Semilog-Linear Behavior and the Setup Factor, A

Many researchers have observed a linear correlation between pile setup and the log of the time elapsed after the EOD. Fig. 1 shows the semilog-linear slope m_Q for setup data presented by Svinkin et al. (1994), including both static and dynamic tests (as did Fellenius et al. 1989). Based on four case histories, from test piles driven in Yolida Clay (Denmark), chalk, and coarse sands, Skov and Denver (1988) proposed a dimensionless setup factor, A, that represents the relative increase in pile capacity per log cycle of elapsed time:

$$\frac{Q}{Q_0} = A \log\left(\frac{t}{t_0}\right) + 1 = \left(\frac{m_Q}{Q_0}\right)\log\left(\frac{t}{t_0}\right) + 1 \quad (1)$$

where A=dimensionless setup factor; Q=whole pile capacity at time t; Q_0=whole pile capacity at initial reference time t_0; t=time elapsed since EOD; t_0=reference time elapsed since EOD; and m_Q=semilog-linear slope of Q versus log-t plot (see Fig. 1).

Fig. 2 shows Svinkin's pile data from Fig. 1 normalized as proposed using t_0=1 day, with the dashed lines defining a range of A=0.25–1.20. Skov and Denver (1988) defined t_0 as the elapsed time at the beginning of the semilog-linear capacity increase. They considered both A and t_0 related to material type and reported A=0.2 for a sand profile with t_0=0.5 days, and A=0.6 for a clay profile with t_0=1 day. However, determination of their onset reference time is difficult, and it affects the value of A by changing the reference capacity, Q_0. Choosing a common reference time for all soils (still within the semilog-linear capacity increase) will help to better define the range of A. For this and the companion paper (Bullock et al. 2005), we used t_0=1 day for driven piles, a practical reference time also used by others.

Furthermore, because Q_0 includes end bearing, which appears to have less setup than side shear, the use of total capacity to determine the setup factor A will lead to a lower and less consistent value than determined from side shear capacity alone. The setup factors presented herein include only the pile side shear capacity (whole pile or segment, stress or force), so that

$$A = \frac{(Q_s/Q_{s0}) - 1}{\log(t/t_0)} \quad \text{(whole pile)} \quad (2)$$

or

$$A = \frac{(F_s/F_{s0}) - 1}{\log(t/t_0)} = \frac{(f_s/f_{s0}) - 1}{\log(t/t_0)} \quad \text{(pile segment)} \quad (3)$$

where A=side shear setup factor (whole pile or pile segment); Q_s ,Q_{s0}=whole-pile side shear (force) at time t or t_0; $F_{s,}$,F_{s0}=pile segment side shear (force) at time t or t_0;

f_s, f_{s0}=unit side shear (stress) at time t or t_0; t=time elapsed since installation; and t_0=reference time, elapsed since installation, =1 day.

Axelsson (1998b) reported $A=0.2-0.8$ using $t_0=1$ day for 235-mm (9.25 in.) concrete piles and 32-mm (1.26 in.) steel rods driven into noncohesive soils. Chow et al. (1996) compiled normalized setup results from a variety of research studies, most of which fall within a similar range. Note that $A=0.2$ appears to represent an approximate minimum value applicable to all of the research results presented. Finally, Camp et al. (1993) documented the setup of 457-mm (18-in.) concrete piles driven in the saturated "Cooper River marl", for both single piles and pile groups. Their research included two different overburden conditions that affected the rate of pore pressure dissipation during and after driving. Both sets of grouped piles had a slightly greater "m_Q" rate of setup than the corresponding single piles, and therefore a higher A value.

Causes of Setup

Many researchers have monitored pore pressures around, or on, a pile installed in low-permeability cohesive soil and found that side shear increased as the driving-induced pore pressures dissipated over a period of a week or longer. According to the conventional pile/soil side shear concept in Eq. (4), SSS could result from either (or both) an increase in the horizontal effective stress, or, as a result of consolidation, an increase in the c'_a or $*'$ strength components:

$$f_s = c'_a + \phi'_h \times \tan \delta' \tag{4}$$

where f_s=unit side shear; c'_a=pile-soil adhesion; ϕ'_h=effective horizontal stress; and δ'=pile-soil drained friction angle.

Karlsrud and Haugen (1985), Lutenegger and Miller (1993), Azzouz and Morrison (1988), Marchetti et al. (1986), and Bond and Jardine (1991) have all shown that the horizontal effective stresses in clays adjacent to the pile start low and increase to some constant level with time, primarily as a result of a decrease in excess pore pressure. However, for piles driven into cohesionless soils, where any excess pore pressure generated during driving should dissipate rapidly (<1 h), setup after dissipation appears to result from causes other than pore pressure changes. Ng et al. (1988) measured changes in the effective horizontal stress against a concrete pile driven into San Francisco sand, both before and after the dissipation of excess pore pressures. Chow et al. (1998) observed an 85% increase in capacity after excess pore pressures should have dissipated around steel pipe piles in Dunkirk sands. They hypothesized, without measurements, that the soil displaced during pile penetration might form a temporary radial arch around the pile, which then relaxed with time, increasing the horizontal effective stresses.

Pore pressure dissipation may explain short-term SSS behavior, predominantly complete within 30 days, but long-term SSS probably results from other causes. Schmertmann (1991) presented examples of time-strength changes in different soil types and argued that these increases resulted from soil restructuring changes, which increased the drained friction angle through "mechanical aging". Axelsson (1998a) concluded that for the long-term setup of piles driven in sand "... the effect of increasing dilatant behavior (due to soil aging) over time was by far the predominant cause." and showed that the dilatant behavior increased both the effective stress at failure and the drained friction angle. The research described herein further investigates these conflicting views.

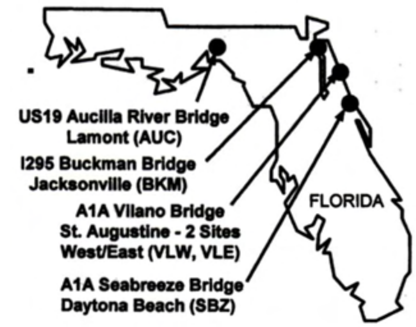

Fig. 3. University of Florida side shear setup test pile sites

University of Florida Side Shear Setup Research Piles

Test Pile Program

The FDOT commonly uses 457-mm (18-in.), square, prestressed, concrete piles to support low-level bridges. UF personnel instrumented and installed dedicated test piles of this type at four bridge construction sites in northern Florida (Fig. 3). Each pile included an O-cell cast into the tip, strain gauges at soil layer boundaries, and total stress cells and pore pressure cells centered in one pile face between adjacent strain gauge elevations. We calculated the shear force and average shear stress acting on the face of the pile from the difference in load between adjacent strain gauge levels. The strain gauges defined a total of 28 side shear segments, 18 of which also included pore pressure and total horizontal stress instrumentation. Subsequent "staged" (repeated) tests over time, provided data to investigate the SSS for each segment. Table 1 summarizes the general information for each test pile. For illustration, this paper presents the Aucilla (AUC) site information (soil conditions, pile construction and instrumentation, driving resistance, and staged O-cell test results). Bullock (1999), and the subsequent FDOT report by McVay et al. (1999), present comprehensive details for all five test piles.

Table 1. Test Pile Summary

Test site	Primary soil type	Pile length (m)	Pile penetration (m)	Date driven
I295 Buckman Bridge Jacksonville, FL	Dense fine sand	10.05	9.16	03/26/94
Aucilla River Bridge US19 (SR20) Aucilla, FL	Soft to med. stiff Si. clay. & Fn. sand	21.33	19.19	03/30/94
Vilano Bridge East AIA, Vilano Beach, FL	Dense fine sand	11.88	10.68	04/14/94
Vilano Bridge West AIA Vilano Beach, FL	Soft to med. stiff silty clay	19.96	18.40	08/24/94
Seabreeze Bridge SR430 EB Daytona Beach, FL	Med. to fn. sand & silty clay	26.84	25.12	01/26/96

Table 2. Research Pile Segment Summary

Test site	Total No. of pile segments for shear setup			No. of pile segments with horizontal effective stress measurement		
	Clay	Mix	Sand	Clay	Mix	Sand
Buckman	0	0	5	0	0	3
Aucilla	3	4	1	3	2	0
Vilano East	0	1	4	0	0	3
Vilano West	2	2	1	2	1	0
Seabreeze	2	0	3	2	0	2
Subtotal	7	7	14	7	3	8
Total		28			18	

Test Program Soils

SPT borings and preliminary cone penetration test soundings at each site provided design information to choose a target tip elevation with adequate bearing for the O-cell and to place the instrumentation cast into each pile. The coastal plain soils at the test sites varied widely, from shelly and silty sands to moderately plastic clays. For analysis purposes, this paper uses three broad soil categories: Sands (S), Clays (C), and Mixed soil (M). "S" includes essentially cohesionless soils, mostly fine sands and silty sands, and some with high shell content. "C" refers to cohesive soils, clays and silty clays with low permeability in which pile penetration should induce significant pore pressure and dissipation. "M" refers to varying mixtures of sand, silt, and clay with some plasticity, as well as thin, intermixed layers of sand, silt, and clay. Table 2 summarizes the pile segments by site, soil type, and the availability of horizontal effective stress measurements.

Test Pile Construction and Instrumentation

This study used the static O-cell test to separate end bearing and side shear, the first such application to driven concrete piles. Use of the O-cells also decreased testing costs, simplified testing, and reduced the required contractor assistance. The schematic in Fig. 4 shows the basic features of the UF research piles, driven to a specified depth to obtain an end-bearing reaction adequate to fail them in side shear. Based on FDOT pile specifications, the first writer (P. J. Bullock) worked with American Fabricating and Equipment Corporation (AEFC) in East Providence, R.I. and Gate Concrete Products Company in Jacksonville, Fla. to design and build the piles for this research. The final design used 12 low-relaxation-steel prestress strands with a diameter of 12.7 mm (0.5 in.), and a concrete strength (28-day compressive) of 41.4 MPa (6,000 psi). Using Type 1 cement, limestone coarse aggregate with a maximum diameter of 19 mm (3/4 in.), a super plasticizer, and a target slump of 150 mm (6 in.), the concrete developed a compressive strength of 58.7 MPa (8,500 psi) at only 14 days.

Fig. 5(a) shows an O-cell sitting above the formwork during pile construction, and Fig. 5(b) shows the added steel reinforcing used to anchor it into the pile bottom. The O-cells, empty and tack-welded shut for transport and driving, had a maximum stroke of approximately 150 mm (6 in.) with a rated load of 2.8 MN (630 kips). AEFC calibrated them to the rated pressure of 69 MPa (10,000 psi) at cell expansions of 25 mm, 76 mm, and 127 mm. Because of a loss of end bearing in sand for the Vilano East pile, a thin steel skirt was added to the Seabreeze (SBZ) and Vilano West (VLW) O-cells to cover the gap that opened between the plates as they separated. Gate Concrete used a small vibrator [Fig. 5(d)] to consolidate the concrete and avoid damaging the instrumentation.

Fig. 6 shows a profile section of the installed instrumentation and soil layering for the AUC pile. Though not commonly used for driven piles, we chose vibrating wire (VW) strain gauges based on their demonstrated long-term reliability (McRae and Simmonds 1991), small size, and economical cost. Installed two per level and tied on opposite sides of the pile between, and parallel to, the two center prestress strands, these strain instruments (Geokon model VCE-4200) had a gauge length of 150 mm (6 in.) and sensitivity of 1 microstrain. They provided strain measurements near the pile tip and at soil layer boundaries established from the prior site investigation.

Used together, the piezometers and Marchetti Dilatometer (DMT) total stress cells measured the effective lateral stress at 20 test pile locations, with three to five locations on each test pile. As shown in Fig. 5(c), we installed each piezometer-DMT pair flush with the top face of the pile (sitting in the form), spaced trans-

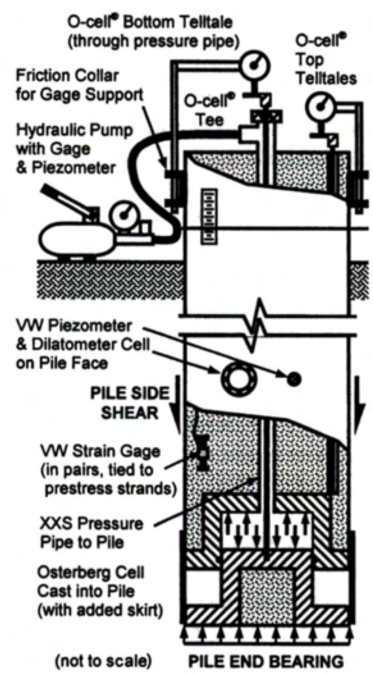

Fig. 4. University of Florida research pile schematic

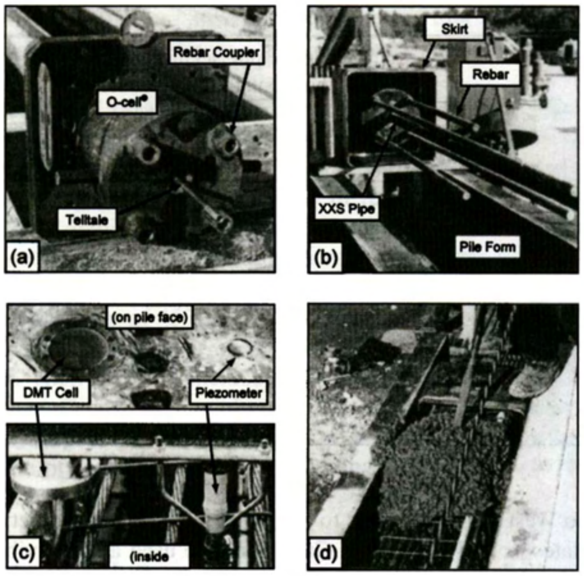

Fig. 5. Research pile construction (a) O-cell with center telltale rod; (b) O-cell sitting over bottom of pile form; (c) dilatometer cell (left) and vibrating wire piezometer (right); and (d) concrete placement

versely 150 mm (6 in.) apart and centered axially between adjacent strain gauge elevations. We used a VW piezometer (Geokon model 4500S) with a 50-μm, 16-mm (5/8-in.) diameter stainless-steel filter, saturated with a solution of 50% glycerin and 50% water and accurate to 5 kPa (0.75 psi) with a 1 MPa (150 psi) range. The DMT cells, copied from the Marchetti DMT blade, had a stainless-steel membrane with a diameter of 60 mm (2.4 in.) and thickness of 0.2 mm (0.008 in.) Manual DMT gauge pressure readings of the membrane lift-off pressure (the DMT "*A-reading*") provided a resolution of about 1 kPa (0.15 psi) and an accuracy of 1 to 4 kPa (0.15 to 0.60 psi) depending on the pressure gauge used. Both the piezometers and DMT cells were covered and sealed during pile construction, and then uncovered during driving. One VW piezometer and one DMT cell (on different pile segments) did not survive the pile construction, but the remaining 18 instrument pairs provided reasonable and consistent measurements throughout the tests.

Two strings of stainless-steel telltale rods, 8 mm (5/16 in.) in diameter and flush coupled in 3-m (10-ft) lengths, provided an unstrained reference down to the tip at opposite corners of the pile to measure pile compression during the load tests. We installed them in polyvinyl chloride telltale pipes (19-mm Schedule 40), filled with oil and capped at the bottom by a steel plate. A third telltale rod, 12.5 mm (1/2 in.) in diameter, threaded into the bottom O-cell plate, and extended up through the cell and pressure pipe, and out a pipe tee with an O-ring seal at the pile top. The telltale rods, installed after driving the pile, remained in place and performed satisfactorily for the duration of this research.

Pile Installation

The bridge contractor at each site drove the research piles using a pile hammer already mobilized for production work: A Fairchild 32 air hammer for the AUC pile and Delmag D46 and D62 diesel hammers for the other four test piles. UF personnel used the Pile Driving Analyzer manufactured by Pile Dynamics, Inc. to monitor pile stresses and capacity during driving. Capacity estimates from the Case Pile Wave Analysis Program (*CAPWAP*) program,

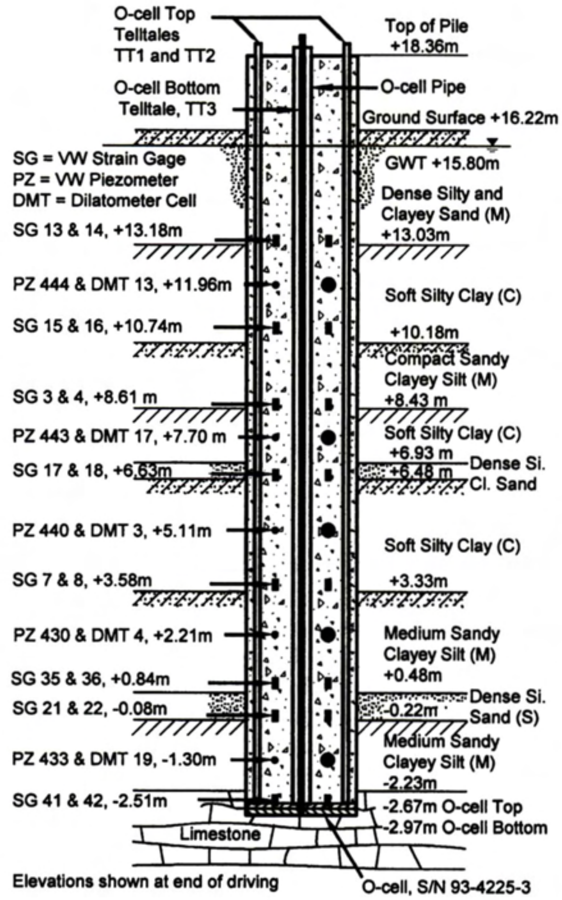

Fig. 6. Aucilla River test pile schematic

based on digitized stress and velocity waves measured during hammer blows from initial driving and subsequent restrikes, provided side shear estimates for the early minutes after driving.

O-Cell Tests

On average, the O-cell tests began within 10 h from the EOD, using a procedure similar to the ASTM D1143 "Quick Test" (ASTM 2000): Approximately 20 load increments to failure, load increased at 4 min intervals, and five to ten unloading increments. The small internal volume of the cells permitted the use of a hand pump to pressurize them from the surface (see Fig. 4), loading the pile from the bottom and failing it upward in side shear. A VW piezometer with 20-kPa resolution (Geokon model 4500H) provided the primary cell pressure measurement, with verification from the pump pressure gauge.

Test personnel used both a wireline and a survey level to measure pile top movement to the nearest 0.25 mm (0.01 in.) using separate scales glued to the pile top. Dial gauges measured the movement of the telltales with respect to the pile top (see Fig. 4), with 0.025-mm (0.001-in.) precision for the bottom telltale and 0.0025-mm (0.0001-in.) precision for the compression telltales. The upward O-cell movement required to achieve side shear failure varied from 3 to 17 mm (0.11 to 6.67 in.). Fig. 7 shows typical load-movement curves from Load Test 5 (LT5) of the AUC pile, with side shear movement plotted upward and the end bearing movement plotted downward. As reported for all of the tests, Fig. 8 shows the net O-cell load, which equals the applied load minus the buoyant weight of the pile.

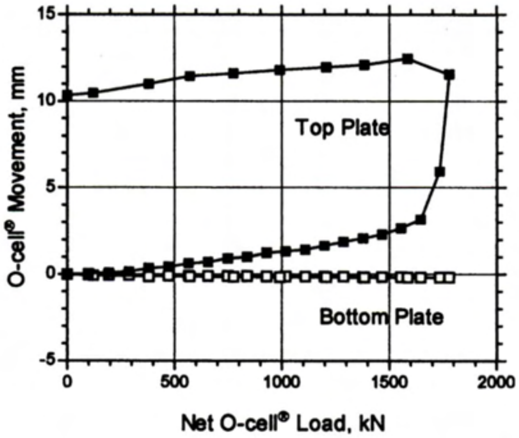

Fig. 7. Load-movement curves, Aucilla River load test 5 (LT5)

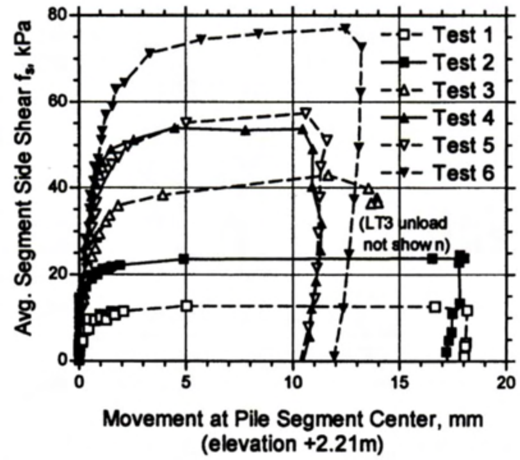

Fig. 9. Aucilla River unit side shear mobilization

After multiplying by the pile stiffness, the average of the strain readings at each gauge elevation provides the pile load. The ratio of the increment of the stress applied by the O-cell to the increment of strain measured just above the O-cell near the failure load of each test provided the best estimate of pile stiffness. Extrapolation of the strain gauge loads near the pile bottom generally agreed well with the applied O-cell load for all tests. Because of the relatively small test strains, we used the same stiffness for all loads during each test. However, the stiffness did increase between 3 and 19% for the five test piles as the concrete aged.

Fig. 8 shows a plot of the pile load versus elevation at the maximum O-cell load for each of the six AUC tests. The slope of these load-transfer plots indicates the amount of side shear acting on the pile. The difference in pile load between adjacent gauge elevations, less the buoyant segment weight, gives the net side shear force acting on that segment (positive downward). Dividing by the segment side area gives the unit side shear. We also averaged the strain readings at the top and bottom of each segment for each load, multiplied this average strain by the segment length, and subtracted the segment compression successively from the pile bottom movement to calculate the axial movement at each strain gage. Fig. 9 shows the mobilization of the unit side shear versus the average movement of each segment for the six static tests of the AUC pile segment centered at elevation +2.21 m. Note that in contrast to the typical top-load pile test, at the end of an O-cell test both the pile top and bottom finish at a zero load condition. This minimizes the creation of residual stresses, which we found negligible except after driving (at the start of the first load test).

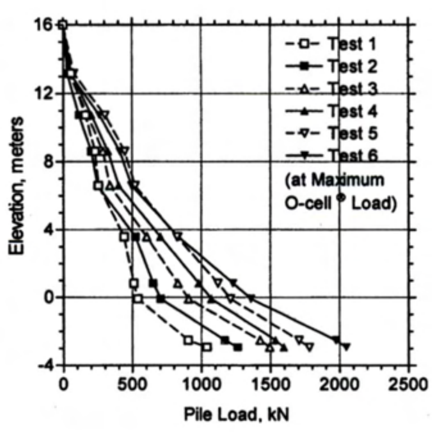

Fig. 8. Aucilla River load transfer curves

The maximum unit side shear developed for each segment during each test provided the basis for the SSS comparisons discussed in the companion paper, (Bullock et al. 2005). Note that the maximum unit side shear for a pile segment does not necessarily occur during the maximum O-cell load at the pile bottom. Segments near the O-cell tended to fail first and then reduce in capacity during later loads, transferring additional load increments farther up the pile.

Variation of Test Results

Experimental data includes both measurement and procedural errors, which cause statistical variation in the test results. For example, the average side shear for each pile segment results from four strain measurements, two at each end of the segment. A small amount of dissimilar soil over each segment, due to natural soil variability and gauge location error, also affects the results. The horizontal effective stress calculated for each pile segment includes errors from both the total pressure cell reading and the subtracted piezometer reading. Located at the segment midheight, these readings may also misrepresent the overall average for the segment. Additional instrumentation would have helped reduce errors, but with added complexity and expense. We believe that we obtained data of sufficient detail and accuracy to achieve our objectives.

University of Florida Test Pile Results

Table 3 summarizes the measured total side shear capacity for each of the static O-cell tests, also shown in Fig. 10. The time elapsed to the final static test on each pile ranged from 16 to 1,727 days after the EOD, with an initial unstaged and then two- to five-staged tests performed in an approximate geometric time progression (1 day, 4 days, 16 days, etc.) to achieve nearly equal spacing on a log time scale. The six O-cell tests at AUC and SBZ required a total expansion of 89 mm (3.5 in) and 72 mm (2.8 in), respectively. Two of the five piles, Vilano Bridge East and VLW, eventually failed in bearing, preventing further side shear failure using only the O-cell.

Although the *CAPWAP* analyses of dynamic tests generally provide reasonably accurate estimates of total capacity, because

Table 3. University of Florida O-cell Test Results

Test site, Q_{s0} at t_0=1 day, setup factor A	Time After EOD t days	Max. sust. load (kN)	Buoy. pile wt. (kN)	Pile side shear: Q_s (kN)	Pile side shear: Q_s/Q_{s0}	O-cell movements at failure: Top (mm)	O-cell movements at failure: Bottom (mm)	O-cell movements at failure: Cum. Exp. (mm)
BKM	0.25	173	40	133	1.00	0.28	−0.25	18.85
Q_{s0}=133kN	3.13	173	40	133	1.00	4.34	−0.13	34.42
A=0.174	15.9	191	40	151	1.14	7.95	−0.76	40.49
	66.0	222	40	181	1.36	3.91	−2.36	50.39
	268	235	40	195	1.47	5.74	−2.77	62.74
AUC	0.98	1039	67	972	1.00	17.17	−3.07	17.27
Q_{s0}=977kN	2.97	1263	67	1197	1.22	4.47	−4.45	38.35
A=0.321	16.1	1494	67	1427	1.46	12.45	−4.75	55.70
	65.1	1595	67	1528	1.56	8.64	−4.52	65.84
	265	1779	67	1712	1.75	11.56	−4.57	76.53
	1727	2049	67	1982	2.03	13.54	−5.51	89.38
VLE	0.32	1223	38	1185	0.94	4.45	−2.29	15.01
Q_{s0}=1257kN	3.93	1382	38	1344	1.07	3.35	−9.93	27.76
A=0.118	15.9	1475	38	1437	1.14	2.79	−26.75	54.56
	77.0	940	38	E.B. Failure	—	1.07	−49.89	92.56
VLW	0.26	469	62	407	0.87	6.45	−1.57	20.80
Q_{s0}=469kN	2.84	581	62	519	1.10	8.66	−3.61	39.24
Q_{s0}=469kN	19.0	697	62	635	1.35	3.63	−19.69	71.02
A=0.292	157	845	62	783	1.67	6.38	−2.92	86.56
SBZ	0.35	1554	84	1471	0.88	9.36	−1.69	13.56
Q_{s0}=1662kN	4.03	2000	84	1916	1.15	7.06	−4.64	21.39
A=0.165	17.9	2221	84	2138	1.29	9.57	−5.33	32.26
	69.9	2291	84	2207	1.33	5.76	−5.27	37.01
	293	2448	84	2365	1.42	6.55	−6.99	54.33
	1057	2446	84	2362	1.42	16.00	−9.04	72.11

Note: Movements (+) up and (−) down; EOD=End of driving; Q_{s0} at t_0=1 day interpolated versus log time; BKN=Buckman Bridge test site; AUC =Aucilla River test site; VLE=Vilano Bridge East test site; VLW=Vilano Bridge West test site; SBZ=Seabreeze Bridge test site.

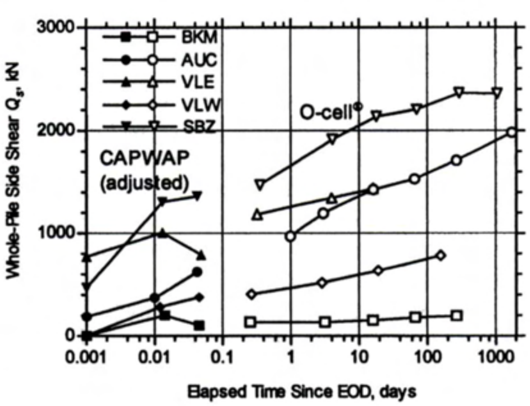

Fig. 10. University of Florida pile side shear capacity

of the numerous input variables we found the separation of the end bearing and side shear components less reliable, especially near the pile tip where side shear and end bearing mobilization overlap. However, as discussed above, the end bearing should not change significantly with time. Any change in total capacity should result mostly from side shear only, thus establishing the approximate linear slope (m_Q) of the side shear versus the logarithm of elapsed time. By adjusting the *CAPWAP* end bearing for each pile to one constant value for all of the dynamic tests (see Table 4), the dynamic and static shear estimates form the roughly continuous log-linear progression shown in Fig. 10. As found in the literature examples above, dynamic tests seem to provide a usable alternative to static tests for checking SSS behavior.

On average, all test piles showed approximate semilog-linear SSS behavior. The dynamic and static test results from the UF research piles confirm a linear trend of side shear versus the logarithm of time. Table 4 also shows, after interpolating for the side shear at t_0=1 day, the whole-pile SSS factors calculated using least-squares regression and Eq. (2). Fig. 11 shows the UF SSS data bounded within the range of A=0.1 to 0.4, less than the expected range of A=0.2 to 0.8 found in the literature.

Table 4. University of Florida *CAPWAP* Results

Test site	Time after EOD, t (min)	(days)	Type of blow 4	Pile tip elev. (m)	*CAPWAP* capacity Side shear (kN)	End bearing (kN)	Total (kN)	Adj. capacity End bearing (kN)	Side shear (Q_{s_1} kN)
BKM	1	0.001	EOD	−4.62	876	961	1837	1837	0
	20	0.014	BOR	−4.69	873	1164	2037	1837	200
	65	0.045	BOR	−4.74	882	1058	1939	1837	102
AUC	1	0.001	EOD	−2.37	683	705	1388	1200	188
	15	0.010	BOR	−2.41	870	700	1570	1200	370
	60	0.042	BOR	−2.51	1045	778	1824	1200	624
VLE	1	0.001	EOD	−9.53	1274	1399	2673	1900	773
	18	0.013	BOR	−9.54	1450	1454	2905	1900	1005
	69	0.048	BOR	−9.57	1401	1290	2691	1900	791
VLW	1	0.001	EOD	−16.90	286	259	545	540	5
	17	0.012	BOR	−16.92	465	356	821	540	281
	65	0.045	BOR	−17.00	495	422	916	540	376
SBZ	1	0.001	EOD	−22.63	703	766	1470	1000	470
	19	0.013	BOR	−22.76	1379	925	2304	1000	1304
	61	0.042	BOR	−22.84	1775	587	2362	1000	1362

Note: EOD=End of driving ($t \approx 1$ min), BOR=Beginning of restrike; BKM=Buckman Bridge test site; AUC=Aucilla River test site; VLE=Vilano Bridge East test site; VLW=Vilano Bridge West test site; SBZ=Seabreeze Bridge test site.

Summary

1. The available literature shows that displacement piles exhibit SSS behavior in a variety of soil types, but with different possible causes.
2. UF researchers successfully drove five 457-mm (18-in.), square prestressed concrete piles at four different sites in Florida, tested them dynamically, performed *CAPWAP* analyses, and subsequently tested and stage-tested them statically using Osterberg cells. Each pile test series included from three to six static tests, with 16 to 1,727 days total setup time.
3. An O-cell cast into each pile tip permitted isolation of the pile side shear. Test measurements included pile compression, pile top and bottom movements, pile strain, pore pressure, total horizontal stress, and (by subtraction) effective horizontal stress against the side of the pile.
4. The test piles provided a total of 28 pile segments for SSS analysis in a variety of soil types. Eighteen segments included measurement of the horizontal effective stress at their midheight.
5. Both the UF setup tests and previous research by others, mostly from staged tests, indicate that the side shear resistance against a driven displacement pile.
6. Using a dimensionless SSS factor A to describe the semilog-linear change of side shear versus time, the UF piles show whole-pile SSS factors $A=0.12$ to 0.32, lower than the range of 0.2 to 0.80 found in the literature.
7. As reported by others, the UF research piles show that static and dynamic test results exhibit a similar linear trend of side shear versus the logarithm of time.

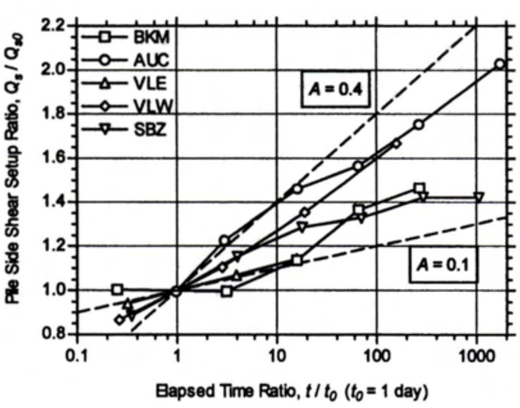

Fig. 11. University of Florida pile side shear setup ratios

Acknowledgments

The National Science Foundation provided primary funding for this project with substantial assistance from the FDOT, the FHWA, and Schmertmann and Crapps, Inc. FDOT Districts 1, 2, 3, and 5 provided valuable assistance in arranging the installation of the test piles in conjunction with on-going bridge projects, and field testing support for the site investigations. The following FDOT Engineers helped facilitate this research: Mr. William Knight, Dr. Sastry Putcha, Mr. Chandra Samakur, Mr. Jon Foshee, Mr. Tom Malerk, Dr. Ching Kuo, Ms. Terry Puckett, and Mr. Peter Lai.

Notation

The following symbols are used in this paper:

A = dimensionless setup factor (semilog-linear slope);
A_s = pile side area;
c'_a = pile-soil adhesion;
F_s, F_{s0} = pile segment side shear (force) at time t or t_0;
f_s, f_{s0} = unit side shear (stress) at time t or t_0;
m_Q = semilog-linear slope of pile capacity versus log of elapsed time;
Q, Q_0 = pile capacity at time t or t_0;
Q_s, Q_{s0} = whole-pile side shear (force) at time t or t_0;
RMX = pile driving analyzer static pile capacity estimate;
t = time elapsed since end of driving;
t_0 = reference time elapsed since end of driving;
δ' = pile-soil drained friction angle; and
ϕ'_h = effective horizontal stress.

References

Airhart, T. P., Hirsch, T. J., and Coyle, H. M. (1967). "Pile-soil system response in clay as a function of excess pore water pressure and other soil properties." *Research Rep. No. 33-8*. Texas Transportation Institute, Texas A&M Univ., College Station, Tex.

American Society for Testing and Materials. (2000). "Standard test method for piles under static axial compressive load." *D 1143-81, Annual Book of ASTM Standards*. ASTM, Philadelphia, 4:08, 96–106.

Axelsson, G. (1998a). "Long-term setup of driven piles in noncohesive." Licentiate thesis, Dept. of Civil and Environmental Engineering, Royal Institute of Technology, Stockholm, Sweden.

Axelsson, G. (1998b). "Long-term setup of driven piles in noncohesive soils evaluated from dynamic tests on penetration rods." *Proc., 1st Int. Conf. on Site Characterization*, P. K. Robertson and P. W. Mayne, eds., Balkema, Brookfield, Vt., 2, 895–900.

Azzouz, A. S., and Morrison, J. M. (1988). "Field measurements on model pile in two clay deposits." *J. Geotech. Eng.*, 114(1), 104–121.

Bond, A. J., and Jardine, R. J. (1991). "Effects of installing displacement piles in a high OCR clay." *Geotechnique*, 41(3), 341–363.

Bullock, P. J. (1999). "Pile friction freeze: A field and laboratory study." PhD dissertation, Dept. of Civil Engineering, Univ. of Florida, Gainesville, Fla.

Bullock, P. J., Schmertmann, J. H., McVay, M. C., and Townsend, F. C. (2005). "Side shear setup. II Results from Florida test piles." *J. Geotech. Geoenviron. Eng.*, 131(3), 301–310.

Camp, W. M., Wright, W. B., and Hussein, M. (1993). "The effect of overburden on pile capacity in a calcareous marl." *Proc., 18th Annual Members' Conf.*, Deep Foundations Institute, Englewood Cliffs, N.J.

Chow, F. C., Jardine, R. J., Brucy, F., and Nauroy, J. F. (1996). "The effects of time on the capacity of pipe piles in dense marine sand." *Proc., 28th Annual Offshore Technology Conf.*, Offshore Technology Conference, Houston, Tex.

Chow, F. C., Jardine, R. J., Brucy, F., and Nauroy, J. F. (1998). "Effects of time on capacity of pipe piles in dense marine sand." *J. Geotech. Geoenviron. Eng.*, 124(3), 254–264.

Fellenius, B. H., Riker, R. E., O'Brien, A. J. O., and Tracy, G. R. (1989). "Dynamic and static testing in soil exhibiting set-up." *J. Geotech. Eng.*, 115(7), 984–1001.

Karlsrud, K., and Haugen, T. (1985). "Axial static capacity of steel model piles in overconsolidated clays." *Proc., 11th Int. Conf. on Soil Mechanics and Foundation Engineering*, Balkema, Brookfield, Vt., 3, 1401–1406.

Kehoe, S. P. (1989). "An analysis of time effects on the bearing capacity of driven piles." *Master's Rep.* Dept. of Civil Engineering, Univ. of Florida, Gainesville, Fla.

Lutenegger, A. J., and Miller, G. A. (1993). "Evaluation of dilatometer method to determine axial capacity of driven model pipe piles in clay." *Proc., Design and Performance of Deep Foundations: Piles and Piers in Soil and Soft Rock*. ASCE, Reston, Va., 41–63.

Marchetti, S., Totani, G., Campanella, R. G., Robertson, P. K., and Taddei, B. (1986). "The DMT-σ_{hc} method for piles driven in clay." *Proc., Use of In Situ Tests in Geotechnical Engineering*, Clemence, ASCE, Reston, Va., 765–779.

McRae, J. B., and Simmonds, T. (1991). "Long-term stability of vibrating wire instruments: One manufacturer's perspective." *Proc., 3rd Int. Symposium on Field Measurements in Geomechanics*. G. Sørum, ed., Balkema, Brookfield, Vt., 283–293.

McVay, M. C., Schmertmann, J., Townsend, F., and Bullock, P. (1999). "Pile friction freeze: A field and laboratory study." *Research Rep. No. WPI 0510632*, Florida Department of Transportation, Tallahassee, Fla.

Ng, E. S., Tsang, S. K., and Auld, B. C. (1988). "Pile foundations: The behavior of piles in cohesionless soils." *Report No. FHWA-RD-88-081*, Federal Highway Administration, McLean, Va.

Preim, M. J., March, R., and Hussein, M. (1989). "Bearing capacity of piles in soils with time dependent characteristics." *Proc., 3rd Int. Conf. on Piling and Deep Foundations*, J. B. Burland and J. M. Mitchell, eds., Balkema, Brookfield, Vt., 363–370.

Samson, L., and Authier, J. (1986). "Change in pile capacity with time: Case histories." *Can. Geotech. J.*, 23(2), 174–180.

Schmertmann, J. H. (1991). "The mechanical aging of soils." *J. Geotech. Eng.*, 117(9), 1285–1330.

Seidel, J. P., Haustorfer, I. J., and Plesiotis, S. (1988). "Comparison of static and dynamic testing for piles founded into limestone." *Proc., 3rd Int. Conf. on the Application of Stress-Wave Theory to Piles*, B. G. Fellenius, ed., BiTech Publishers, Vancouver, BC, 717–723.

Shioi, Y., Yoshida, O., Meta, T., and Homma, M. (1992). "Estimation of bearing capacity of steel pipe pile by static loading test and stress-wave theory." *Proc., 4th Int. Conf. on the Application of Stress-Wave Theory to Piles*, F. B. S. Barends, ed., Balkema, Brookfield, Vt., 325–330.

Skov, R., and Denver, H. (1988). "Time-dependence of bearing capacity of piles." *Proc., 3rd Int. Conf. on the Application of Stress-Wave Theory to Piles*, B. G. Fellenius, ed., BiTech Publishers, Vancouver, BC, 879–888.

Svinkin, M. R., Morgano, C. M., and Morvant, M. (1994). "Pile capacity as a function of time on clayey and sandy soils." *Proc., 5th Int. Conf. on Piling and Deep Foundations*, Deep Foundations Institute, Englewood Cliffs, N.J., 1.11.1–1.11.8.

Tavenas, F., and Audy, R. (1972). "Limitations of the driving formulas for predicting the bearing capacities of files in sand." *Can. Geotech. J.*, 9(1), 47–62.